

Non-existence of self-similar solutions containing a black hole in a universe with a stiff fluid or scalar field or quintessence

Tomohiro Harada^{1,2,*}, Hideki Maeda^{1,3,4,†} and B. J. Carr^{5,6,‡}

¹*Department of Physics, Rikkyo University, Tokyo 171-8501, Japan,* ²*Department of Physics, Kyoto University, Kyoto 606-8502, Japan,* ³*Graduate School of Science and Engineering, Waseda University, Tokyo 169-8555, Japan,* ⁴*Department of Physics, International Christian University, Mitaka, Tokyo 181-8585, Japan,* ⁵*Research Center for the Early Universe, Graduate School of Science, University of Tokyo, Tokyo 113-0033, Japan,* ⁶*Astronomy Unit, Queen Mary, University of London, Mile End Road, London E1 4NS, UK*

(Dated: June 24, 2018)

We consider the possible existence of self-similar solutions containing black holes in a Friedmann background with a stiff fluid or a scalar field. We carefully study the relationship between the self-similar equations in these two cases and emphasize the crucial role of the similarity horizon. We show that there is no self-similar black hole solution surrounded by an exact or asymptotically flat Friedmann background containing a massless scalar field. This result also applies for a scalar field with a potential, providing the universe is decelerating. However, if there is a potential and the universe is accelerating (as in the quintessence scenario), the result only applies for an exact Friedmann background. This extends the result previously found in the stiff fluid case and strongly suggests that accretion onto primordial black holes is ineffective even during scalar field domination. It also contradicts recent claims that such black holes can grow appreciably by accreting quintessence. Appreciable growth might be possible with very special matter fields but this requires *ad hoc* and probably unphysical conditions.

PACS numbers: 04.70.Bw, 97.60.Lf, 04.25.Dm, 95.35.+d

I. INTRODUCTION

Scalar fields are one of the key ingredients in modern cosmology. They play an important role during inflation and certain phase transitions; they feature in the preheating and quintessence scenarios; and they are pervasive in all sorts of alternative theories (eg. string theory and scalar-tensor theory) which are likely to be relevant in the high curvature phase of the early Universe. In such scenarios, it is often assumed that scalar fields dominated the energy of the Universe at some stage of its evolution. This could have profound implications for the formation and evolution of any primordial black holes (PBHs) that may have formed in the early Universe [1]. It would also modify the constraints on the number of PBHs provided by various observations [2, 3].

A particularly interesting example of this arises if the dark energy which generates the cosmic acceleration observed at the present epoch is associated with a quintessence field. In this context, it has recently been claimed [4, 5] that PBHs could grow enough through accreting quintessence to provide seeds for the sort of supermassive black holes thought to reside in galactic nuclei [6]. This claim is based on a simple Newtonian

analysis, in which a PBH with size comparable to the cosmological particle horizon appears to grow in a self-similar manner [7], i.e. its size is always the same fraction of the size of the particle horizon. This suggests that PBHs may accrete surrounding mass very effectively if their initial size is fine-tuned. However, this analysis neglects the cosmological expansion [8, 9]. More recently, a general relativistic analysis of this problem has been applied for a black hole accreting dark energy and phantom energy [10, 11, 12], as well as a ghost condensate [13, 14]. However, the cosmological expansion is still neglected in these analyses.

The possibility of spherically symmetric self-similar PBH solutions was first studied more than 30 years ago for a fluid with a radiation equation of state ($p = \epsilon/3$) [8]. This study was also prompted by the Newtonian analysis and demonstrated analytically that there is no self-similar solution which contains a black hole attached to an exact Friedmann background via a sonic point (i.e. in which the black hole forms by purely causal processes). The Newtonian analysis is therefore definitely misleading in this case. There are self-similar solutions which are *asymptotically* Friedmann at large distances from the black hole. However, these correspond to special initial conditions, in which matter is effectively thrown into the black hole at every distance; they do not contain a sonic point because they are supersonic everywhere.

Similar results were subsequently proved for all perfect fluid systems with equation of state of the form $p = k\epsilon$ with $0 < k < 1$ [15, 16, 17]. Indeed it was shown that

*Electronic address:harada@rikkyo.ac.jp

†Electronic address:hideki@gravity.phys.waseda.ac.jp

‡Electronic address:B.J.Carr@qmul.ac.uk

the only physical self-similar solution which can be attached to an external Friedmann solution via a sonic point is Friedmann itself; the other solutions either enter a negative mass regime or encounter another sonic point where the pressure gradient diverges [16]. Later numerical relativistic calculations have confirmed that PBHs cannot accrete much for these perfect fluid systems [18, 19, 20, 21, 22, 23, 24]. It has also been shown that the asymptotically Friedmann self-similar solutions with black holes are not strictly Friedmann at infinity, because they exhibit a solid angle deficit which could in principle show up in the angular diameter test [25].

The limiting values of k require special consideration. In the $k = 0$ case, there is no sonic point, so the uniqueness is trivial; again there are asymptotically Friedmann self-similar solutions with PBHs but only for special initial conditions [8]. The stiff fluid case ($k = 1$) is more complicated and has an interesting history. It was originally claimed by Lin et al. [26] that there *could* exist a self-similar black hole solution in this case but subsequent calculations by Bicknell and Henriksen [27] showed that this solution does not contain a black hole after all because the alleged event horizon is timelike. The only way to avoid this conclusion would be if the fluid turned into null dust at this timelike surface, but this seems physically implausible. It therefore appears that there is no self-similar solution containing a black hole in an exact Friedmann background for any value of k in the range [0,1].

In view of the prevalence of scalar fields in the early Universe, it is clearly important to know whether the non-existence of a self-similar solution extends to the scalar field case. One might expect this from the stiff fluid analysis, since a scalar field is equivalent to a stiff fluid provided the gradient is everywhere timelike [28]. This is supported by recent numerical studies of the growth of PBHs in a scalar field system, which - for a variety of initial conditions - give no evidence for self-similar growth [29, 30]. However, it is very difficult to determine through numerical simulations whether self-similar growth is impossible for any specific initial data. One therefore needs an *analytic* proof that there is no self-similar black hole solution if the cosmological expansion is taken into account. This paper presents such a proof and also provides the basis for studying the growth of black holes in an expanding universe containing more general matter fields.

The plan of this paper is as follows. In Section II, we review the stiff fluid case, with particular emphasis on the earlier work of Lin et al. [26] and Bicknell and Henriksen [27]. In Section III, we consider the massless scalar field case, using Brady's formulation of the self-similar equations as an autonomous system [31] and making a detailed comparison with the stiff fluid case. We prove that there is no self-similar solution unless the behaviour of the matter is very contrived. In Section IV we extend the analysis to the case of a scalar field with an exponential potential (as applies in the quintessence scenario) and

show that the proof applies in this case also. We summarize our conclusions in Section V. Various technical issues are relegated to appendices, including a comparison with previous literature, a discussion of the global characteristics of these solutions, and an analysis of the behaviour of solutions at the similarity horizon. We use geometrised units with $c = G = 1$ throughout this paper.

II. STIFF FLUID CASE

A. Bicknell and Henriksen's formulation

First, we show how a stiff fluid description of a scalar field can give insight into the fluid-field correspondence for self-similar solutions [32]. A stiff fluid is a perfect fluid with the equation of state $p = \epsilon$ and stress-energy tensor

$$T^{ab} = \epsilon(2u^a u^b + g^{ab}). \quad (2.1)$$

If u^a is vorticity-free, one can show that this matter field is equivalent to a massless scalar field ϕ , for which the stress-energy tensor is

$$T_{ab} = \phi_{,a}\phi_{,b} - \frac{1}{2}g_{ab}\phi_{,c}\phi^{,c} \quad (2.2)$$

and the gradient $\phi_{,a}$ is timelike. The associated energy density and 4-velocity are

$$\epsilon = -\frac{1}{2}\phi_{,c}\phi^{,c}, \quad u_a = \pm \frac{\phi_{,a}}{\sqrt{-\phi_{,c}\phi^{,c}}}, \quad (2.3)$$

where the sign in the second equation is chosen so that u^a is future-directed. The line element in a spherically symmetric spacetime can be written as

$$ds^2 = -e^{2\nu(t,R)} dt^2 + e^{2\lambda(t,R)} dR^2 + r^2(t,R)(d\theta^2 + \sin^2\theta d\phi^2), \quad (2.4)$$

where R and r are the comoving and area radial coordinates, respectively.

Let us now assume self-similarity (i.e. the homothetic condition), which implies that we can write

$$\nu = \nu(X), \lambda = \lambda(X), S(X) = \frac{r}{R}, \phi = h(X) - \kappa \ln|t|, \quad (2.5)$$

where $X \equiv \ln(R/|t|)$. The constant κ is arbitrary but we will need to assume $\kappa = 1/\sqrt{12\pi}$ below in order to allow the Friedmann solution. If we adopt comoving coordinates, which is always possible providing the 4-velocity is timelike, then T^μ_ν is diagonal. In this case, $h(X)$ must be constant and so ϕ depends only on t .

Following Ref. [16], we now introduce the following variables:

$$V^2 = e^{2\lambda-2\nu+2X}, \quad E = 8\pi\epsilon R^2, \quad A = \frac{m}{4\pi\epsilon r^3}, \quad (2.6)$$

where V is the speed of the fluid flow relative to the similarity surface $X=\text{const}$, m is the Misner-Sharp mass,

E is a dimensionless measure of the energy density and A is one third of the ratio of the average density within r to the local density there. Energy conservation yields the following integrals:

$$e^{2\nu} = a_\nu E^{-1} e^{2X}, \quad e^{2\lambda} = a_\lambda E^{-1} S^{-4}, \quad (2.7)$$

where a_ν and a_λ are constants of integration. Eqs. (2.3), (2.5) and (2.6) give

$$e^{2\nu} = 4\pi\kappa^2 E^{-1} e^{2X}, \quad (2.8)$$

so a_ν is identified as $4\pi\kappa^2$ and is invariant under rescaling of t and R . If we rescale R appropriately, we can also set a_λ to be $4\pi\kappa^2$. Eqs. (2.6) and (2.7) then imply [27]

$$V^2 = S^{-4}, \quad (2.9)$$

so the Einstein field equations reduce to the following autonomous system [27, 32]:

$$(V^2)' = 2(1 - A)V^2, \quad (2.10)$$

$$A' = \frac{1}{2}(1 + A)(1 - 3A) - 2AV^2 \frac{A - 4\pi\kappa^2}{1 - V^2}, \quad (2.11)$$

$$E' = 2 \left[V^2 \frac{A - 4\pi\kappa^2}{1 - V^2} + 1 \right] E, \quad (2.12)$$

together with a constraint equation

$$V^2(1 - A)^2 - (1 + A)^2 + 16\pi\kappa^2 V^2 (E^{-1} |V| - A) = 0. \quad (2.13)$$

Here a prime denotes a derivative with respect to X .

B. $V^2 = 1$ surface

Once we have determined initial values satisfying Eq. (2.13), Eqs. (2.10) and (2.11) constitute a two-dimensional autonomous system and Eq. (2.12) can be evolved freely. However, Eq. (2.11) shows that the condition $V^2 = 1$ corresponds to a singular point in the above system of differential equations, so the usual uniqueness of solutions may not apply. This is because one may have a sonic point where $V^2 = 1$ and, in the stiff fluid case, this coincides with a null surface; we term this a ‘‘similarity horizon’’.

In order to understand the significance of the similarity horizon, it is useful to draw the Penrose diagram for the self-similar black hole spacetime. This is shown in Fig. 1, which is also equivalent to Figure 5 of [33]. It can be obtained by combining the Penrose diagrams for a decelerating flat Friedmann universe, which is discussed in Appendices B and C, and that for a naked singularity [34]. The spacetime is asymptotically flat Friedmann with a spacelike big bang singularity outside the particle horizon. It also has a null naked singularity, a spacelike black hole singularity and a black hole event horizon. The

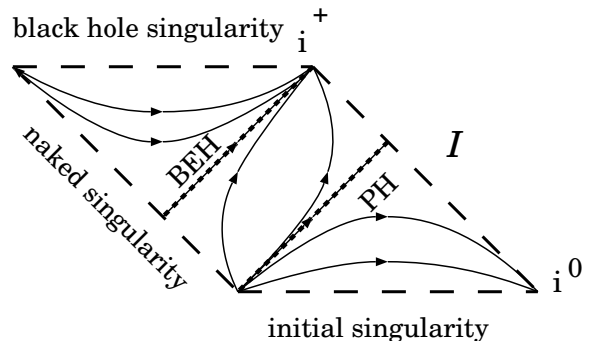


FIG. 1: The causal structure of self-similar black holes in a decelerating universe. The trajectories of similarity surfaces are shown. There is a spacelike big bang singularity, a null naked singularity and a spacelike black hole singularity. The particle horizon (PH) and black hole event horizon (BEH) are both similarity horizons.

similarity surfaces are spacelike outside the particle horizon and inside the black hole event horizon, timelike in between and null on the horizons themselves. This shows that the particle horizon and black hole event horizon both correspond to similarity horizons.

We note that the induced metric on the $X = \text{const}$ surface can be written as

$$ds^2 = -e^{2\nu}(1 - V^2)dt^2 + r^2(d\theta^2 + \sin^2\theta d\phi^2). \quad (2.14)$$

If this surface is null, it can be identified with the black hole event horizon or the cosmological particle horizon, both corresponding to the condition $V^2 = 1$ providing ν remains finite. If the gradient of the energy density is finite at the similarity horizon, Eq. (2.12) also requires $A = 4\pi\kappa^2$. This coincidence between singular points of the ordinary differential equations (ODEs), i.e. sonic points, and similarity horizons only applies for a stiff fluid. Sonic points are timelike surfaces for perfect fluids with the equation of state $p = k\epsilon$ ($0 < k < 1$).

If one wants a solution which represents a black hole surrounded by the exact Friedmann solution, we first note that the velocity gradient must be positive on both sides of the matching surface. (This is a consequence of the fact that the Friedmann sonic point is a node, as discussed in Section III E.) Therefore $V^2(X)$ must have the behaviour shown in Fig. 2. As X decreases from infinity, V^2 first decreases, goes below 1, reaches a minimum, then increases and reaches 1 again. The first point where V^2 crosses 1 is the particle horizon, $X = X_{\text{ph}}$. One might expect the second point where V^2 crosses 1 to be the black hole event horizon, $X = X_{\text{beh}}$, and indeed Lin et al. [26] make this interpretation. However, Bicknell and Henriksen [27] showed that this is not the case: the similarity surface is timelike rather than null because ν diverges there. More precisely, E goes to 0, which shows that the gradient of the scalar field is null, and the factor $e^{2\nu}(1 - V^2)$ in Eq. (2.14) tends to a finite positive limit, which shows that the second crossing surface is timelike.

This reveals the limitation of the comoving-coordinate framework for scalar field systems. The Lin et al. and Bicknell and Henriksen analyses are discussed in more detail in Appendix A.

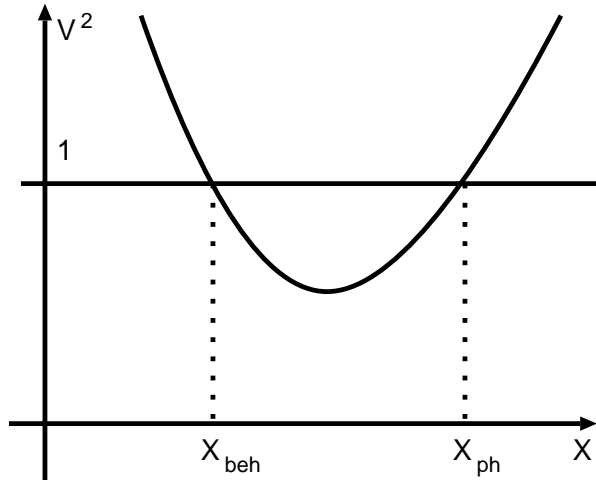


FIG. 2: The required behaviour of the velocity function $V^2(X)$ for a black hole solution which is attached to an exact Friedmann background.

Because Bicknell and Henriksen could only find a solution in which V^2 has the required behaviour up to the point where $V^2 = 1$, they inferred that no black hole solution is possible if the fluid has the same equation of state everywhere. However, they did find that a black hole solution is possible if the stiff fluid turns into null dust at the surface where $V^2 = 1$. This situation is obviously contrived, so in this paper we seek a more physical extension with a massless scalar field.

III. MASSLESS SCALAR FIELD CASE

A. Brady's formulation

Let us now return to the original scalar field description, in which the stress-energy tensor is given by Eq. (2.2). If we adopt (non-comoving) Bondi coordinates (v, r) , where v is advanced time, the metric can be written as

$$ds^2 = -g\bar{g}dv^2 + 2gdvdr + r^2(d\theta^2 + \sin^2\theta d\phi^2), \quad (3.1)$$

where g and \bar{g} are functions of v and r . This applies whether the gradient of the scalar field is timelike, null or spacelike. In this coordinate system, for a self-similar solution we can take the independent variable to be $\xi \equiv \ln(r/|v|)$ and then define the following variables:

$$\begin{aligned} y(\xi) &= \frac{\bar{g}}{g} = 1 - \frac{2m}{r}, & z(\xi) &= \bar{g}^{-1}x, \\ \phi &= \bar{h}(\xi) - \kappa \ln|v|, & \gamma(\xi) &= \dot{\bar{h}}(\xi), \end{aligned} \quad (3.2)$$

where $x = r/v = \pm e^\xi$ has the same sign as v and a dot denotes a derivative with respect to ξ . Note that ϕ depends on ξ in this case, because we are not using comoving coordinates. The quantity z will play an analogous role to the quantity V in the stiff fluid picture. The quantity γ is related to the gradient of the scalar field; the field itself never appears explicitly in the equations.

With the self-similarity ansatz, the Einstein equations and equations of motion for the scalar field reduce to the following ODEs:

$$(\ln g) \dot{} = 4\pi\dot{\bar{h}}^2, \quad (3.3)$$

$$\dot{\bar{g}} = g - \bar{g}, \quad (3.4)$$

$$g \left(\frac{\dot{\bar{g}}}{g} \right) = 8\pi(\dot{\bar{h}} + \kappa)[x(\dot{\bar{h}} + \kappa) - \bar{g}\dot{\bar{h}}], \quad (3.5)$$

$$(\bar{g}\dot{\bar{h}}) \dot{} + \bar{g}\dot{\bar{h}} = 2x \left(\dot{\bar{h}} + \ddot{\bar{h}} + \kappa \right). \quad (3.6)$$

We then have an autonomous system [31]:

$$\dot{z} = z(2 - y^{-1}), \quad (3.7)$$

$$\dot{y} = 1 - (4\pi\gamma^2 + 1)y, \quad (3.8)$$

$$(1 - 2z)\dot{\gamma} = 2\kappa z - \gamma(y^{-1} - 2z), \quad (3.9)$$

with the constraint equation

$$y[(1 + 4\pi\kappa^2) - 4\pi(\gamma + \kappa)^2(1 - 2z)] = 1. \quad (3.10)$$

Note from Eq. (3.2) that $y < 1$ if the Misner-Sharp mass is positive. This system was investigated in the context of cosmic censorship in [35] and, for $\kappa = 0$, one has the exact Roberts solution [36]. Eq. (3.10) gives two values of γ for each (y, z) :

$$\gamma = -\kappa \pm \sqrt{\frac{1 + 4\pi\kappa^2 - y^{-1}}{4\pi(1 - 2z)}}, \quad (3.11)$$

with the positive (negative) branch corresponding to positive (negative) values of $\gamma + \kappa$. The structure of this system of equations is the same as in the stiff fluid description. Since Eq. (3.11) gives γ in terms of y and z , once we have determined initial values satisfying the constraint (3.10), Eqs. (3.7) and (3.8) together with Eq. (3.11) form a two-dimensional dynamical system and Eq. (3.9) is evolved freely.

Special physical significance is associated with the gradient of the scalar field being null. This is because the scalar field can no longer be identified with a stiff fluid once the gradient has turned from timelike to spacelike. Since this gradient is

$$\phi^c\phi_{,c} = -\gamma y[2z(\gamma + \kappa) - \gamma]r^{-2}, \quad (3.12)$$

it can become null under three conditions: $y = 0$, $\gamma = 0$ and $2z(\gamma + \kappa) = \gamma$. From Eq. (3.10), the condition $\gamma = 0$ gives

$$z = \frac{1 - y}{8\pi\kappa^2 y}, \quad (3.13)$$

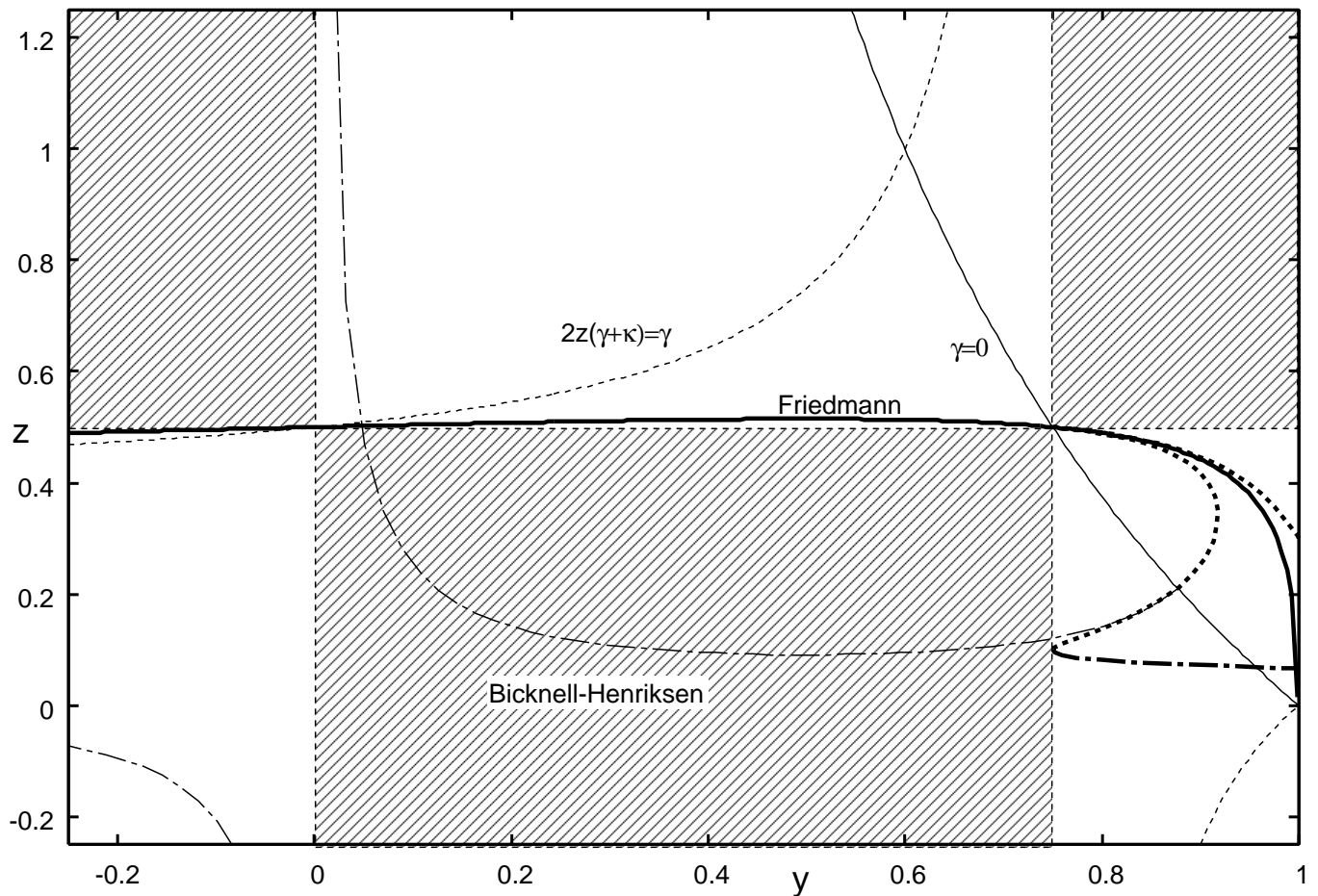


FIG. 3: The solutions in the yz plane for $4\pi\kappa^2 = 1/3$. The shaded regions are prohibited for a real scalar field. The expanding flat Friedmann solution is plotted as a thick solid line, the curve $\gamma = 0$ as a thin solid line, and the curve $2z(\gamma + \kappa) = \gamma$ as a thin dashed line. The gradient of the scalar field can change from timelike to spacelike on the last two curves and also on $y = 0$. Note that the parts of the $2z(\gamma + \kappa) = \gamma$ and $\gamma = 0$ curves in $z > 1/2$ correspond to the null conditions for different solution branches but are shown together for convenience. The flat Friedmann solution has a cosmological apparent horizon at $(y = 0, z = 1/2)$, a particle horizon at $(y = 3/4, z = 1/2)$ and ends at $(y = 1, z = 0)$. Two numerical solutions within the particle horizon are shown by the thick dotted lines. The upper one is a positive branch and goes directly to the negative mass region ($y > 1$). The lower one reaches $y = 3/4$, where it is converted from the positive branch to the negative branch (shown by the thick dashed-dotted line) before going to the negative mass region. The Bicknell-Henriksen null-dust black hole solution, which connects to the lower numerical solution, is indicated by a thin dashed-dotted line, but this is never realized by a scalar field. The black hole has an event horizon where the solution intersects $z = 1/2$ and an apparent horizon at $(y = 0, z = \infty)$.

which always corresponds to the positive branch of Eq. (3.11). From Eq. (3.10), the condition $2z(\gamma + \kappa) = \gamma$ gives

$$z = \frac{1 - y}{2[1 - (1 + 4\pi\kappa^2)y]}. \quad (3.14)$$

Since $\gamma + \kappa = \kappa/(1 - 2z)$, this corresponds to the positive (negative) branch of Eq. (3.11) for $z < (>)1/2$. These three conditions for the gradient of the scalar field to be null are shown in Fig. 3 for $\kappa = 1/\sqrt{12\pi}$. Note that the positive and negative branches of Eq. (3.11) should not really be represented in the same yz diagram, since the conditions $\gamma = 0$ and $2z(\gamma + \kappa) = \gamma$ clearly cannot be satisfied simultaneously, but we do so for convenience.

If the gradient is spacelike, the energy density ϵ given by Eq. (2.3) is negative. This is not unphysical (eg. the weak energy condition is always satisfied), even though the identification with a stiff fluid is no longer possible. However, γ must be real and, from Eq. (3.10), this applies within three regions in the yz plane:

$$z > \frac{1}{2} \quad \text{and} \quad 0 < y < \frac{1}{1 + 4\pi\kappa^2},$$

or

$$z < \frac{1}{2} \quad \text{and} \quad y > \frac{1}{1 + 4\pi\kappa^2},$$

or

$$z < \frac{1}{2} \quad \text{and} \quad y < 0.$$

These are the three unshaded regions in Fig. 3. Although one might speculate that the complex γ region could be associated with a complex scalar field, this cannot be confirmed within the context of the present single-field analysis.

B. Similarity and trapping horizons

From Eqs. (3.1) and (3.2), the induced metric on the surface $\xi = \text{const}$ is

$$ds^2 = -y^{-1}z^{-2}(1-2z)dr^2 + r^2(d\theta^2 + \sin^2\theta d\phi^2). \quad (3.15)$$

Thus, providing $y \neq 0$, $z = 1/2$ corresponds to a similarity horizon and this is either a particle horizon or an event horizon. Although $z = 1/2$ plays a similar role in the field description to $V^2 = 1$ in the fluid description, we will show that the degeneracy in the fluid description is resolved in the field description. From Eq. (3.10), γ can be finite at $z = 1/2$ only if $y = 1/(1 + 4\pi\kappa^2)$.

If $y = 0$, one has a trapping horizon. This notion was defined in [37, 38] and has turned out to be a very useful generalization of the concept of apparent horizons. Past trapping horizons include cosmological apparent horizons, while future ones include black hole apparent horizons. Equation (3.10) implies that either z or γ must diverge when $y = 0$. From Eqs. (3.1) and (3.2), $dr/dv = \bar{g}/2 = e^\xi/(2z)$ is an outgoing null surface, so a future trapping horizon has infinite $|z|$ and finite γ , while a past trapping horizon has $z = 1/2$ and infinite γ . More precisely, $y \propto z^{-1}$ in the vicinity of future trapping horizons, while $y \propto (1 - 2z)$ and $\gamma \propto y^{-1}$ in the vicinity of past trapping horizons, where we have used Eq. (3.10). In the latter case, the apparent singularity arises from the fact that ξ or r has an extremum along ingoing null rays $v = \text{const}$ on past trapping horizons.

From these properties of similarity and trapping horizons, we can deduce the following. A similarity horizon with $z = 1/2$ cannot be a future trapping horizon. $z = 1/2$ is satisfied at both similarity and past trapping horizons. We can show that a black hole event horizon is untrapped with negative ingoing null expansion and positive outgoing null expansion, where we need to assume the existence of future null infinity for the definition of a black hole event horizon. This is because, if both expansions were negative, no causal curve in the past neighbourhood of the black hole event horizon could reach future null infinity. On the other hand, if both expansions were positive, there would exist a causal curve in the future neighbourhood of the black hole event horizon which could reach future null infinity. It also follows that a black hole event horizon cannot coincide with a past trapping horizon. Therefore, a black hole event horizon is untrapped, i.e. its null expansions have different signs.

C. Transformation between the two formulations

The key step is to obtain the correspondence between two equivalent expressions for the three quantities $2m/r$, $8\pi\epsilon r^2$ and V . The first two can be written as

$$2m/r = AE|V|^{-1} = 1 - y, \quad (3.16)$$

$$8\pi\epsilon r^2 = E|V|^{-1} = 4\pi\gamma y[2z(\gamma + \kappa) - \gamma]. \quad (3.17)$$

To obtain the expression for V in the field description, we introduce the following vector fields:

$$\bar{u}_a = \phi_{,a}, \quad \bar{n}_a = \epsilon_a^b \phi_{,b}, \quad (3.18)$$

where ϵ_{ab} is the totally antisymmetric tensor, which satisfies $\epsilon_a^c \epsilon_{cb} = -g_{ab}$. Since these two vectors satisfy the normalisation relation

$$\bar{u}_a \bar{u}^a = -\bar{n}_b \bar{n}^b, \quad (3.19)$$

the velocity function V can be written as

$$V = -\frac{\bar{n}^a \xi_a}{\bar{u}^a \xi_a} \quad (3.20)$$

if $\phi_{,a}$ is timelike; here $\xi^a \equiv (\partial_\xi)^a$. Since ξ is a function of X , this definition applies for any self-similar spacetime with a scalar field. Calculating the right-hand side of this equation in the Bondi coordinates and assuming $\kappa \neq 0$, we have

$$V = 1 + \left(2 - \frac{1}{z}\right) \frac{\gamma}{\kappa}, \quad (3.21)$$

where ϵ^{01} is chosen to be positive. These relations give the explicit coordinate transformations between the fluid and field descriptions if $\phi_{,a}$ is timelike.

Equation (3.21) means that the condition $V^2 = 1$ in the fluid description separates into two independent conditions, $z = 1/2$ and $\gamma = 0$, in the field description. From Eq. (3.15), the condition $z = 1/2$ implies that the $\xi = \text{const}$ surface is null unless $y = 0$. On the other hand, from Eq. (3.12), the condition $\gamma = 0$ implies $\phi_{,a}$ is null and this is plotted in Fig. 3 using Eq. (3.13). There is no coordinate singularity even when $\phi_{,a}$ is null in the field description, and this is very important for the present analysis. As γ approaches zero, Eqs. (2.8), (3.17) and (3.21) imply that $1 - V^2$ is proportional to γ and that $e^{2\nu}(1 - V^2)$ has a finite limit $e^{2X}(1 - 2z)/(yz^2)$. This is zero only if $z = 1/2$, so Eq. (2.14) implies that the similarity surface is null only in this case.

D. Friedmann solution

We now consider the flat Friedmann solution. This has $A = 1/3$ everywhere in the fluid description and a regular similarity horizon. Since $4\pi\kappa^2 = 1/3$, Eqs. (2.10)–(2.12) imply

$$V^2 = C^2 e^{4X/3}, \quad A = \frac{1}{3}, \quad E = \frac{3}{4} C^3 e^{2X}. \quad (3.22)$$

The integration constant C comes from the remaining rescaling freedom of t . Using Eqs. (3.10), (3.16), (3.17), (3.21) and (3.22), it can be shown that the Friedmann solution is described by:

$$z = 3 \frac{\sqrt{1-y}(1-\sqrt{1-y})}{y(1+2\sqrt{1-y})} \quad (\text{expansion}), \quad (3.23)$$

$$z = \frac{\sqrt{1-y}(1+\sqrt{1-y})}{y(1+2\sqrt{1-y})} \quad (\text{collapse}). \quad (3.24)$$

The discussion about trapping horizons confirms that the first and second solutions represent the expanding and collapsing Friedmann solutions, respectively. The expanding solution is shown by the thick solid line in Fig. 3 and this crosses $z = 1/2$ at $y = 0$ and $y = 3/4$. From Eq. (3.21) $V = 1$ at $y = 3/4$ and so this corresponds to the cosmological particle horizon. Eq. (3.23) implies $y^{-1}(1-2z) \rightarrow -1/12$ as $y \rightarrow 0$, which leads to $V = 2$ from Eqs. (3.11) and (3.21). Therefore this surface is spacelike and corresponds to a past trapping horizon. This is the cosmological apparent horizon, which is outside the particle horizon and coincides with the Hubble horizon [9]. This illustrates that the condition $z = 1/2$, like the condition $V = 1$, does not always correspond to a null surface. The causal structure of the Friedmann solution in this case is shown in Appendix B.

E. Structure of similarity horizons

As we have seen, a similarity horizon is defined as a null similarity surface. It is denoted by $\xi = \xi_s$ and characterized by $z = 1/2$ and $y \neq 0$. Since this corresponds to a singular point of the autonomous system (3.7)–(3.9), the usual uniqueness of solutions may break down there. The behaviour of solutions around $\xi = \xi_s$ can be analysed by dynamical systems theory [16, 32, 39]. First, we restrict our attention to $\kappa \neq 0$ and assume that γ has a finite limit at $\xi = \xi_s$. Then $(1-2z)\dot{\gamma}$ tends to zero at the similarity horizon from Eq. (3.9). Otherwise, $\gamma \propto \ln|\xi - \xi_s|$ in the vicinity of $\xi = \xi_s$ and this necessarily implies a spacetime singularity unless $y = 0$.

The full details of the analysis are described in Appendix D. Here we describe the important qualitative results. The regularity of the similarity horizon requires

$$y_s = \frac{1}{1+4\pi\kappa^2}, \quad \gamma_s = \frac{1}{4\pi\kappa}, \quad (3.25)$$

from Eqs. (3.9) and (3.10). We linearise the ODEs around the similarity horizon and represent the solutions as trajectories in (z, y, γ, ξ) space. Generically regular solutions can only cross the similarity surface along two directions in this space, corresponding to two eigenvectors \mathbf{e}_1 and \mathbf{e}_2 . The associated values of $\dot{\gamma}_s$ are:

$$\dot{\gamma}_1 = \kappa \frac{(1-\alpha)(1+\alpha)}{\alpha^2(1-2\alpha)}, \quad \dot{\gamma}_2 = \pm\infty \quad (3.26)$$

where $\alpha \equiv 4\pi\kappa^2$. Along the second eigenvector, there is a solution which describes a density discontinuity surface at fixed $\xi = \xi_s$. We call this a shock-wave solution.

As discussed in Appendix D, the signs of the eigenvalues associated with the two eigenvectors determine the qualitative behaviour of solutions around the equilibrium point. For $0 < 4\pi\kappa^2 < 1/2$, the similarity horizon is a non-degenerate node, with \mathbf{e}_1 and \mathbf{e}_2 corresponding to the secondary and primary directions, respectively. This means that there is a one-parameter family of solutions which belong to the \mathbf{e}_2 direction and an isolated solution which belongs to the \mathbf{e}_1 direction. In particular, this includes the case with $4\pi\kappa^2 = 1/3$. Since the flat Friedmann solution is along \mathbf{e}_1 , this is isolated, while all other solutions have a sound-wave with diverging $\dot{\gamma}$ at the similarity horizon. One of them is a shock-wave. For $4\pi\kappa^2 = 1/2$, the similarity horizon is a degenerate node. For $1/2 < 4\pi\kappa^2 < 1$, it again becomes a non-degenerate node but with \mathbf{e}_1 and \mathbf{e}_2 corresponding to the primary and secondary directions, respectively. For $4\pi\kappa^2 > 1$, the similarity horizon is a saddle point. This means that there are two isolated solutions associated with \mathbf{e}_1 and \mathbf{e}_2 .

Brady [31] has analysed the structure of the system governed by Eqs. (3.7)–(3.10) for all values of the constant κ . For $0 < 4\pi\kappa^2 < 1$, which includes our choice of $4\pi\kappa^2 = 1/3$, the allowed region in the yz plane is similar to that shown in Fig. 3. The solution can cross $z = 1/2$ with finite γ only if y_s and γ_s are given by Eq. (3.25). Brady has also made a non-linear analysis of the similarity horizon and we expand his analysis in Appendix E, correcting a typographical error. A comparison of the two analyses shows that the qualitative behaviour obtained by linearizing the ODEs reflects the true non-linear behaviour.

F. Non-existence of self-similar PBHs with a massless scalar field

If the initial perturbation extends to infinity, so that the specific binding energy is negative there, the perturbation never goes to zero because the angular part of the metric acquires a numerical factor which results in a solid angle deficit [25]. Although these solutions are sometimes described as asymptotically Friedmann [8], they could in principle be observationally distinguished from the exact Friedmann solution by the angular diameter test. However, inflation itself would not produce models of this kind. We therefore first seek a black hole solution surrounded by an exact flat Friedmann solution beyond the sonic point, which is also the particle horizon, and consider matching to other interior self-similar solutions there.

The required behaviour of the function z for a black hole is shown by the solid line in Fig. 4. As we move along the ingoing null surface $v = \text{const}$ from the cosmological apparent horizon, ξ decreases from ξ_{cah} . Thus

$z(\xi)$ increases from $1/2$, reaches a maximum, turns to decrease and then crosses $1/2$ at ξ_{ph} . Up to this point, the solution is described by the Friedmann solution, but the uniqueness of the solution breaks down at ξ_{ph} . Because the Friedmann solution approaches the similarity horizon along a secondary direction, it has to connect to a member of the one-parameter family of solutions associated with the primary direction. As we decrease ξ further, in order to have a black hole solution, z should first decrease, reach a minimum, begin to increase and then cross $1/2$ at the black hole event horizon $\xi = \xi_{\text{beh}}$. It should then diverge at the black hole apparent horizon $\xi = \xi_{\text{ah}} < \xi_{\text{beh}}$ (which is necessarily within the event horizon), although this feature is not required for the following discussion.

It is easy to see that the required behaviour is impossible. Because $z < 1/2$ is required for $\xi_{\text{beh}} < \xi < \xi_{\text{ph}}$, we need $y > 3/4$ to avoid the shaded region in Fig. 3 and Eq. (3.7) then implies $2/3 < \dot{z}/z < 2$. However, this means that z cannot have an extremum, which gives a contradiction. The solution therefore either enters the negative mass region beyond $y = 1$ or approaches $z = 0$ as $\xi \rightarrow -\infty$ (i.e. as $r \rightarrow 0$), corresponding to the exact Friedmann solution. The only way to invalidate this proof would be to find a solution which goes through the lower shaded region in Fig. 3. One can never reach the black hole event horizon by going around this region.

Figure 3 shows solutions obtained through numerical integration of Eqs. (3.7) – (3.9) inside the particle horizon. Some solutions directly cross $y = 1$ and go into the negative mass region with $y > 1$. However, there are also solutions which reach $y = 3/4$ at $z < 1/2$. These necessarily cross the curve $\gamma = 0$, which means that they have the required behaviour for V^2 in Fig. 2 but not for z in Fig. 4. One could also consider solutions which pass smoothly into the region where the scalar field gradient is spacelike. However, in this case, the above proof still applies because z remains monotonic, so there is again no black hole solution. Such solutions have to touch the line $y = 3/4$, after which they become negative-branch solutions and eventually enter the negative mass region with $y > 1$.

Although we have assumed that the spacetime exterior to the black hole solution is an exact Friedmann solution, the proof also applies if it is asymptotically Friedmann. For the equality $4\pi\kappa^2 = 1/3$ must still be satisfied in order to allow the exact Friedmann solution, the black hole solution must still have a particle horizon at $z = 1/2$ and there must still be a region where $0 < z < 1/2$ inside the particle horizon. Therefore one can still conclude that z cannot cross $z = 1/2$ again from below. This proves that there is no black hole event horizon inside the particle horizon even for asymptotically Friedmann solutions.

It should be noted that the situation is quite different for a perfect fluid with equation of state $p = k\rho$ ($0 \leq k < 1$). In fact, in this case, analytic and numerical studies show that there *do* exist asymptotically Friedmann self-

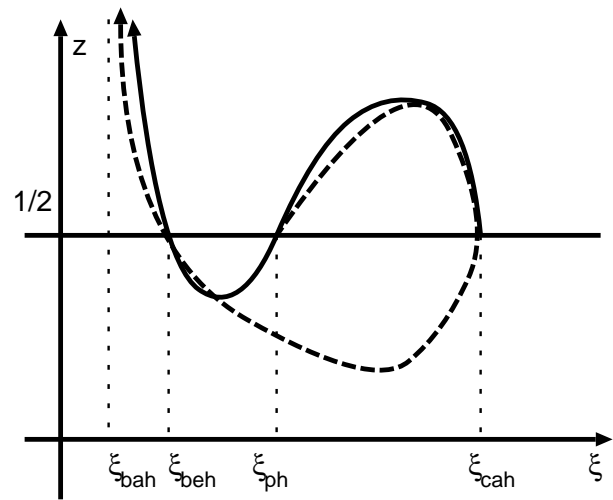


FIG. 4: The required form of $z(\xi)$ for a black hole solution is plotted as a solid line if the cosmological apparent horizon is spacelike and as a dashed line if it is timelike.

similar solutions with a particle horizon and black hole event horizon [8, 16, 17]. The crucial point is that there is no extremum in z as a function of ξ in a subsonic region but there can be in a supersonic but subluminal ($z < 1/2$) region for $0 \leq k < 1$. The reason why the non-existence proof works in the scalar case is that the sonic horizon in the scalar field system coincides with the similarity horizon. Since z cannot have an extremum in a subluminal region, the non-existence of self-similar black holes in the scalar field system follows immediately.

If there is a shock-wave, it can be located only at the similarity horizon. As we have seen, such a solution has $z = 1/2$ and $y = (1 + 4\pi\kappa^2)^{-1}$ but changing γ . If we consider a solution which is interior to this shock-wave and assume a regular junction, it must also have $z = 1/2$ and $y = (1 + 4\pi\kappa^2)^{-1}$ there. Because of regularity, γ must have the same value $(4\pi\kappa)^{-1}$ at the similarity horizon and in the interior solution. In fact, this shows that no regular shock-wave is allowed. We can still have a sound-wave solution with diverging $\dot{\gamma}$ for $0 < 4\pi\kappa^2 < 1/2$, which is included in the above proof. If we do not assume regularity of the similarity horizon, we may consider an extension beyond the similarity horizon to a solution with a different κ . However, the different value of κ means a different value of y for $z = 1/2$ because $y = (1 + 4\pi\kappa^2)^{-1}$ there. One needs a singular null hypersurface because of the discontinuity in the Misner-Sharp mass. We do not consider this possibility further here.

G. Bicknell and Henriksen's PBH construction with a null dust

Bicknell and Henriksen [27] found an extension of the self-similar stiff fluid solution beyond the timelike $V^2 = 1$ surface, containing null dust. The extension is given by

an ingoing Vaidya solution [40], in which the line element is given by

$$ds^2 = - \left(1 - \frac{2m(v)}{r} \right) dv^2 + 2dvdr + r^2(d\theta^2 + \sin^2\theta d\phi^2). \quad (3.27)$$

The stress-energy tensor for null dust can be written in the form

$$T_{ab} = \sigma l_a l_b, \quad (3.28)$$

where l_a is a null vector. For the Vaidya solution, $l_a = -\delta_a^0$ and σ is written as

$$\sigma = \frac{1}{4\pi r^2} \frac{dm}{dv}. \quad (3.29)$$

The similarity assumption implies

$$m(v) = \mu v, \quad (3.30)$$

where μ is an arbitrary constant. Then, in terms of y , z and ξ , Eqs. (3.2) and (3.16) imply that this solution is

$$y = 1 - 2\mu e^{-\xi}, \quad (3.31)$$

$$z = \frac{e^\xi}{1 - 2\mu e^{-\xi}}. \quad (3.32)$$

Eliminating ξ , we have

$$z = \frac{2\mu}{y(1-y)}. \quad (3.33)$$

The junction between the Vaidya metric and the stiff fluid solution can be implemented on the line $\gamma = 0$, given by Eq. (3.13). For $4\pi\kappa^2 = 1/3$, we then have

$$\mu = \frac{3}{4}(1 - y_*)^2, \quad (3.34)$$

where $y = y_*$ on the junction surface. Thus $0 < \mu < 3/64$ for $3/4 < y_* < 1$. We can see explicitly from Eqs. (3.7) and (3.8) that \dot{z} and \dot{y} are continuous on this surface, which guarantees the continuity of the first and second fundamental forms of the junction surface. For the extended solution to have a black hole event horizon, we require that z go below $1/2$ for $y > 0$ and Eq. (3.33) shows that this condition is necessarily satisfied. An example of an extended solution is shown by a thin dashed-dotted line in Fig. 3.

If the massless scalar field ϕ has a null gradient, the stress-energy tensor (2.2) is equivalent to that for the null dust (3.28), with $l_a = \sigma^{-1/2} \nabla_a \phi$. For this reason, one might expect that this construction could be realised consistently with a massless scalar field alone. Nevertheless, this is not true. If a null dust is equivalent to a massless scalar field, the vorticity-free condition must be satisfied:

$$\nabla_{[a}(\sqrt{\sigma} l_{b]}) = 0. \quad (3.35)$$

However, for the Vaidya solution, we can see

$$\nabla_{[0}(\sqrt{\sigma} l_{1]}) = -\frac{\sqrt{\sigma}}{r}. \quad (3.36)$$

This means that the vorticity-free condition is not satisfied for the Vaidya solution unless it is vacuum. Therefore, the null dust which appears in the Vaidya metric cannot be realized by a massless scalar field.

The stiff fluid or massless scalar field in this construction turns into null dust on the timelike surface where $\gamma = 0$, but it is then no longer describable as a massless scalar field. The Bicknell and Henriksen PBH solution exploits this feature and that is why this solution goes through the prohibited region where γ is complex and why it circumvents the above proof that z cannot have a minimum. However, this may be regarded as physically contrived.

IV. SCALAR FIELD WITH A POTENTIAL

A. Autonomous system

When the scalar field ϕ has a potential $V(\phi)$, the existence of self-similar solutions requires it to be of exponential form [41]:

$$V(\phi) = V_0 e^{\sqrt{8\pi}\lambda\phi}. \quad (4.1)$$

Then the stress-energy tensor of the scalar field is

$$T_{ab} = \phi_{,a}\phi_{,b} - g_{ab} \left(\frac{1}{2} \phi_{,c}\phi^{,c} + V_0 e^{\sqrt{8\pi}\lambda\phi} \right). \quad (4.2)$$

With the self-similarity ansatz, the Einstein equations and the equations of motion for the scalar field reduce to the following ODEs:

$$(\ln g) \dot{} = 4\pi \dot{\bar{h}}^2, \quad (4.3)$$

$$\dot{\bar{g}} = g \left(1 - 8\pi x^2 V_0 e^{\sqrt{8\pi}\lambda\bar{h}} \right) - \bar{g}, \quad (4.4)$$

$$g \left(\frac{\dot{\bar{g}}}{g} \right) = 8\pi(\dot{\bar{h}} + \kappa)[x(\dot{\bar{h}} + \kappa) - \bar{g}\dot{\bar{h}}], \quad (4.5)$$

$$(\dot{\bar{g}}\dot{\bar{h}}) + \bar{g}\dot{\bar{h}} = \sqrt{8\pi}\lambda g x^2 V_0 e^{\sqrt{8\pi}\lambda\bar{h}} + 2x \left(\dot{\bar{h}} + \ddot{\bar{h}} + \kappa \right), \quad (4.6)$$

where we use the same notations as for the massless case, except that one requires $\kappa = (\sqrt{2\pi}\lambda)^{-1}$ in the presence of a potential. This system has been investigated in the context of the kink instability analysis [42].

We define the functions y , z and γ in the same way as before [cf. Eq. (3.2)] and introduce a new function

$$\beta \equiv 8\pi V_0 \exp \left(2\xi + \frac{2\bar{h}}{\kappa} \right). \quad (4.7)$$

Eqs. (3.7)–(3.10) are then replaced by

$$\dot{z} = z[2 - y^{-1}(1 - \beta)], \quad (4.8)$$

$$\dot{y} = 1 - \beta - (4\pi\gamma^2 + 1)y, \quad (4.9)$$

$$(1 - 2z)\dot{\gamma} = 2\kappa z - \gamma[y^{-1}(1 - \beta) - 2z] + \frac{\beta}{4\pi\kappa y} \quad (4.10)$$

$$\dot{\beta} = 2\beta \left(1 + \frac{\gamma}{\kappa} \right) \quad (4.11)$$

with the constraint equation

$$y[(1 + 4\pi\kappa^2) - 4\pi(\gamma + \kappa)^2(1 - 2z)] = 1 - \beta. \quad (4.12)$$

The solutions are therefore constrained to lie on a 3-dimensional hypersurface in a 4-dimensional phase space. Because the dimension of the phase space is higher than that for the massless case, the analysis becomes more complicated. However, the number of degrees of freedom for the self-similar solutions is the same because the parameter κ is fixed by the potential, whereas it is freely chosen for the massless case.

B. Friedmann solution

The flat Friedmann solution satisfies these equations providing $\kappa = (\sqrt{2\pi\lambda})^{-1}$. This is in contrast to the massless case, in which the Friedmann solution requires $4\pi\kappa^2 = 1/3$. In the presence of a potential, the scale factor is given by

$$a(t) \propto t^{4\pi\kappa^2} \propto t^{2/\lambda^2}. \quad (4.13)$$

Thus the expansion is decelerated for $0 < 4\pi\kappa^2 < 1$, accelerated for $4\pi\kappa^2 > 1$ and with a constant velocity for $4\pi\kappa^2 = 1$. We call the scalar field in the accelerated case a ‘‘quintessence’’ field. As discussed in Appendix B, there are five types of causal structures, corresponding to $0 < 4\pi\kappa^2 < 1/2$, $4\pi\kappa^2 = 1/2$, $1/2 < 4\pi\kappa^2 < 1$, $4\pi\kappa^2 = 1$ and $4\pi\kappa^2 > 1$.

C. Structure of similarity horizons

As seen in Section III B, similarity horizons are characterised by $z = 1/2$ and $y \neq 0$, future trapping horizons by $y = 0$ and $|z| = \infty$, and past trapping horizons by $y = 0$ and $z = 1/2$. From Eqs. (4.10) and (4.12), the regularity of the similarity horizon yields

$$y_s = \frac{1 - \beta_s}{1 + 4\pi\kappa^2}, \quad \gamma_s = \frac{\beta_s + 4\pi\kappa^2}{16\pi^2\kappa^3(1 - \beta_s)}, \quad (4.14)$$

where we have assumed $\beta_s \neq 1$. Eq. (4.12) shows that $\beta_s = 1$ is only possible when $\gamma = \infty$, which means that the similarity horizon coincides with the past trapping horizon. Note that Eq. (4.14) reduces to Eq. (3.25) when $\beta_s = 0$.

As is before, we linearise the ODEs around the similarity horizon, which again corresponds to a singular point in the presence of a potential. The situation is qualitatively similar to the massless case, except that the solutions are now represented as trajectories in $(z, y, \gamma, \xi, \beta)$ space. Generically regular solutions can only cross the similarity surface along two eigenvectors \mathbf{e}_1 and \mathbf{e}_2 . As before, these are associated with a finite and infinite value of $\dot{\gamma}_s$, respectively. We do not give the analogue of Eq. (3.26) explicitly, since it is very complicated, but

the infinite value is associated with a shock-wave solution, for which $y = y_s$, $z = 1/2$, $\beta = \beta_s$, $\xi = \xi_s$ but γ changes. This belongs to the one-parameter family of solutions which cross the similarity horizon along \mathbf{e}_2 . As before, the similarity horizon behaves as a node for $0 < 4\pi\kappa^2 < 1$ or as a saddle for $4\pi\kappa^2 > 1$. Appendix F provides the details of the linearised ODEs and eigenvectors for this case.

D. Non-existence of self-similar PBH in decelerating Friedmann universe

We now consider solutions which are exactly Friedmann outside the particle horizon. The Friedmann background is decelerating for $0 < 4\pi\kappa^2 < 1$, i.e. for a steep potential with $\lambda^2 > 2$. As shown in Appendix B, the particle horizon in this case is a similarity horizon and the Penrose diagram for a solution containing a black hole would be as indicated in Fig. 1. Because of the nodal nature of the similarity horizon, there is a one-parameter family of interior solutions which can be matched to this background. However, we now show that no interior self-similar solution can contain a black hole event horizon.

For $0 < 4\pi\kappa^2 < 1/2$, i.e. for $\lambda^2 > 4$, the cosmological apparent horizon is spacelike and outside the particle horizon, as shown in Appendix B. So if we have a black hole event horizon, as ξ decreases monotonically along a future-directed ingoing null ray from the particle horizon, z decreases from $1/2$, reaches a minimum, increases and then crosses $1/2$ again. y is positive in this region. The required behaviour of z is therefore as plotted with a solid curve in Fig. 4. For $1/2 < 4\pi\kappa^2 < 1$, i.e. $2 < \lambda^2 < 4$, the cosmological apparent horizon is timelike and inside the particle horizon, as shown in Appendix B. Since a black hole event horizon is untrapped, as ξ decreases monotonically along a future-directed ingoing null ray from the cosmological apparent horizon, z decreases from $1/2$, reaches a minimum, increases and then crosses $1/2$ again. y increases from zero as we move along a future-directed ingoing null ray from the cosmological apparent horizon. The required behaviour of z is plotted with a dashed curve in Fig. 4. For $4\pi\kappa^2 = 1/2$, i.e. $\lambda^2 = 2$, the cosmological apparent horizon coincides with the particle horizon, as shown in Appendix B.

We now show that such a solution cannot exist. From Eqs. (4.8) and (4.12), we have

$$\frac{\dot{z}}{z} = 1 - 4\pi\kappa^2 + 4\pi(\gamma + \kappa)^2(1 - 2z). \quad (4.15)$$

Therefore, if $4\pi\kappa^2 < 1$, z cannot have an extremum for $z < 1/2$. Hence there is no self-similar black hole solution in this case. The proof also applies for the asymptotic Friedmann background. Thus the conclusion that there is no self-similar black hole solution in the case without a potential also applies for a decelerating universe.

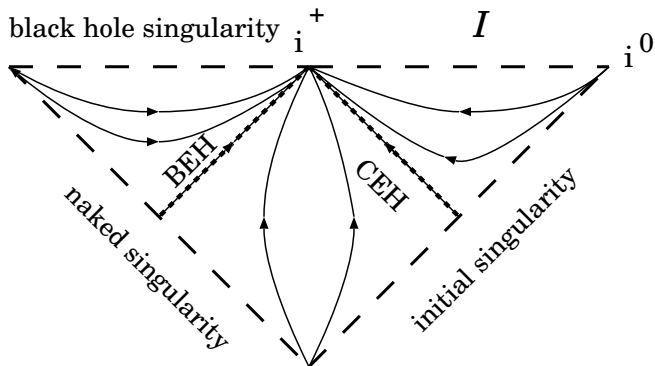


FIG. 5: The causal structure of self-similar black holes in an accelerating universe. The trajectories of similarity surfaces are shown. There is a null big bang singularity, a null naked singularity and a spacelike black hole singularity. The cosmological event horizon (CEH) and the black hole event horizon (BEH) are both null similarity surfaces, i.e., similarity horizons.

E. Non-existence of self-similar PBH in accelerating universe

If $4\pi\kappa^2 = 1$, or $\lambda^2 = 2$, the Friedmann universe expands with a constant speed. In this case, the big bang singularity is an outgoing null surface and future null infinity is ingoing null surface, as shown in Appendix B. We proved in Appendix B that there is no similarity horizon in this case, so we cannot match the exterior Friedmann background to an interior black hole solution. We therefore exclude this case.

For $4\pi\kappa^2 > 1$, i.e. for a flat potential with $0 < \lambda^2 < 2$, the scalar field with a potential acts as dark energy, which causes accelerated expansion. The Penrose diagram for a self-similar black hole spacetime is now different from the decelerating case, as indicated in Fig. 5. This reflects the fact that the causal structure of the flat Friedmann universe is itself modified, as discussed in Appendices B and C. The spacetime now has a null big bang singularity, as well as a null naked singularity, a spacelike black hole singularity and black hole event horizon inside the cosmological event horizon. The similarity surfaces are spacelike outside the cosmological event horizon and inside the black hole event horizon, timelike in between them and null on the horizons themselves. So the similarity horizons can be identified with the cosmological event horizon or black hole event horizon.

In this case, the sign of the right-hand side of Eq. (4.15) is apparently indefinite, so we cannot immediately apply the earlier proof. However, the nature of the similarity horizon in the Friedmann solution now plays a crucial role. Because the cosmological apparent horizon is timelike and inside the cosmological event horizon, as shown in Appendix B, the external Friedmann solution could only be matched to an internal self-similar solution at the cosmological event horizon. As shown in Appendix D,

this horizon is a saddle, so there are just two isolated solutions which can be matched to the Friedmann background solution: one is Friedmann itself and the other is a shock-wave solution. However, since we assume regularity of the cosmological event horizon, z , y and β must be the same in the shock-wave solution and the exterior Friedmann background. The regularity therefore requires the same value of γ and hence this similarity horizon is identical to that of the exterior Friedmann solution. Since the interior can only be the Friedmann solution itself, we can conclude that there is no self-similar black hole solution interior to the Friedmann background. This proof does not exclude the possibility of a self-similar black hole in the asymptotically inflationary Friedmann background and this possibility is now under investigation [43].

V. CONCLUSION

In summary, we have shown that there is no self-similar black hole solution surrounded by an exact flat Friedmann solution for a massless scalar field or a scalar field with a potential. This extends the previous result obtained for a perfect fluid with equation of state $p = k\epsilon$ ($0 \leq k \leq 1$). Indeed we can summarize this important result as a formal theorem.

Theorem. *Let (\mathcal{M}, g) be a spacetime which satisfies the following four conditions: (i) it is spherically symmetric; (ii) it admits a homothetic Killing vector; (iii) it contains a stiff fluid or a scalar field with non-negative potential; (iv) it contains no singular hypersurface. Let (\mathcal{M}, g) also satisfy at least one of the following two conditions: (v) it coincides with the flat Friedmann solution outside some finite radius; (vi) it is asymptotic to the decelerating Friedmann solution. Then (\mathcal{M}, g) has no black-hole event horizon.*

This result disproves recent claims that PBHs could grow self-similarly through accreting a quintessence field. It also suggests that accretion onto black holes is suppressed by the cosmological expansion in a scalar field system. This is consistent with numerical simulations, which show that PBHs with different initial sizes eventually become much smaller than the particle horizon [29, 30]. Note that, for the massless case, it has already been shown analytically that the accretion rate is exactly zero for a black hole whose size is exactly that of the cosmological apparent horizon [29, 30].

Although Bicknell and Henriksen's construction shows that there are self-similar black hole solutions satisfying the necessary energy conditions, such solutions are *ad hoc* and probably not physically realistic. Certainly the PBH mass could grow self-similarly ($M \propto t$) only with very special matter fields. On the other hand, if we drop self-similarity condition, there might still be black hole solutions which exhibit an interesting amount of

accretion. For example, kinematically self-similar solutions [44, 45] contain characteristic scales and this suggests consideration of a wider class of matter fields. In this case, one might have solutions in which the PBH grows as $M \propto t^{1/\alpha}$ ($\alpha \neq 1$) for some similarity index α .

Acknowledgments

TH and HM thank H. Kodama, K. Nakamura, E. Mitsuda and N. Dadhich for helpful discussions and comments. TH thanks T. Nakamura for helpful comments. This work was partly supported by the Grant-in-Aid for Young Scientists (B) 18740144 (TH) and 18740162 (HM) from the Ministry of Education, Culture, Sports, Science and Technology (MEXT) of Japan. BJC thanks the Research Center for the Early Universe at Tokyo University for hospitality during this work. The numerical and algebraic calculations were carried out on machines at YITP in Kyoto University.

APPENDIX A: COMPARISON WITH OTHER WORK

It is interesting to explain why the results of this paper disagree with those presented in various earlier papers. First, we clarify the flaw in the claim by Lin et al. [26] that a self-similar black hole solution can be attached to the Friedmann particle horizon if the equation of state is stiff. This flaw was first pointed out by Bicknell and Henriksen [27] but our analysis has illuminated its nature. Lin et al. use different variables from those in Section II but it is easy to express the results in our notation. They prove analytically that, as the similarity variable X decreases, the function V must reach a minimum below 1 and then rise again to 1 (cf. Fig. 2). They correctly point out that the pressure and velocity gradient diverge at this point but they fail to appreciate that the density function E goes to zero and that the metric function ν goes to infinity, so that the surface $V^2 = 1$ is timelike rather than null. They therefore misinterpret this point as a black hole event horizon. They argue that the divergence of the pressure gradient is non-physical, since it can be removed by introducing an Eddington-Finkelstein-type coordinate, but do not notice that the pressure gradient also diverges at the cosmological particle horizon. However, it is worth stressing that Lin et al. do correctly deduce the form of the solution up to the inner point where $V^2 = 1$.

Second, we point out the source of our disagreement with the claim of Bean and Magueijo [4] that black holes can accrete quintessence fast enough to grow self-similarly. They consider a scalar field in a potential of the form given by Eq. (4.1). By generalizing the analysis of Jacobson [46], which attaches a Schwarzschild solution to a cosmological background in which the field has the asymptotic value ϕ_c , they claim that the energy flux

through the event horizon is $T_{vv} = \dot{\phi}_c^2$, leading to a black hole accretion rate

$$\frac{dM}{dt} = 16\pi M^2 \dot{\phi}_c^2. \quad (\text{A1})$$

They correctly infer that only the kinetic energy of the scalar field is accreted, the scalar potential merely influencing the evolution of the asymptotic background field:

$$\phi_c = \frac{2}{\lambda\sqrt{8\pi}} \log\left(\frac{t}{t_0}\right) \quad (\text{A2})$$

where t_0 is a constant of integration. The accretion rate therefore becomes

$$\frac{dM}{dt} = \frac{KM^2}{t^2} \quad (\text{A3})$$

with $K = 8/\lambda^2$, which can be integrated to give

$$M = \frac{M_0}{1 - \frac{KM_0}{t_0} \left(1 - \frac{t_0}{t}\right)}. \quad (\text{A4})$$

For $M_0 \ll K^{-1}t_0$, corresponding to an initial black hole mass much less than that of the particle horizon, this implies negligible accretion. However, for $M_0 = K^{-1}t_0$, Eq. (A4) predicts a self-similar solution, $M \propto t$, in which the black hole always has the same size relative to the particle horizon. This is the result which Bean and Magueijo exploit. For $M_0 > K^{-1}t_0$, the mass diverges at a time $t = t_0/[1 - t_0/(KM_0)]$.

However, this analysis is exactly equivalent to that of Zeldovich and Novikov [7], which neglects the background cosmological expansion and which Carr and Hawking disproved. Bean and Magueijo caution that the Carr-Hawking proof only applies for a perfect fluid and may not be relevant if the scalar field has a potential. However, the result of this paper confirms that there is no black hole self-similar solution even in this case. (Betwieser and Glatzel [47] also question the Carr-Hawking analysis but they only use a general causality argument and do not give a detailed calculation.) It is interesting to note that a more refined Newtonian analysis (but still neglecting the background expansion) implies that the critical black hole size for self-similar growth exceeds the scale associated with a separate closed universe condition for an equation of state parameter exceeding 0.6 [9]. This also indicates that the Newtonian prediction cannot be correct.

Finally, we comment on the paper by Custodio and Horvath [5]. They also consider black hole accretion of a quintessence field with a scalar potential but, instead of Eq. (A1), obtain

$$\frac{dM}{dt} = 27\pi M^2 \dot{\phi}_c^2, \quad (\text{A5})$$

where the numerical factor differs from that assumed in Eq. (A1) because of relativistic beaming. They disagree

with Bean and Magueijo's choice of the function $\dot{\phi}_c$ on the grounds that it neglects the local decrease in the background scalar field resulting from the accretion. For reasons which are not altogether clear, they therefore prefer to focus on a model in which the quintessence flux into the black hole is constant. This requires that the potential have a specific shape, which is not in fact of the form (4.1) required by self-similarity. This leads to the mass evolution

$$M = \frac{M_0}{1 - \frac{\bar{K}M_0}{t_0}(t - t_0)}, \quad (\text{A6})$$

where \bar{K} is a constant related to the (fixed) flux. Again this is similar to the Zeldovich-Novikov formula. The mass diverges at a time $t = t_0[1 + 1/(\bar{K}M_0)]$, just as Eq. (A4) does for $M_0 > K^{-1}t_0$, and they attribute this unphysical feature to the fact that the assumption of constant mass flux fails. They therefore consider alternative models in which the flux decreases as a power of time.

Although we agree with their conclusion that the Bean-Magueijo argument is wrong, we would claim that Custodio and Horvath have not identified the more significant reason for its failure, namely that it neglects the background cosmological expansion. In general, they find that the increase in the black hole mass is small unless its initial value is finely tuned. However, according to the result in this paper, even the latter claim is misleading.

APPENDIX B: GLOBAL STRUCTURE OF FRIEDMANN SOLUTION

Since we are considering the possibility of black holes in a Friedmann background, we briefly review the global structure of the flat Friedmann solution. This has the metric

$$ds^2 = -dt^2 + a^2(t)[d\chi^2 + \chi^2(d\theta^2 + \sin^2\theta d\phi^2)] \quad (\text{B1})$$

with the scale factor $a(t) = Ct^q$, where C and q are positive constants. The domain of the variables is $0 < t < \infty$ and $0 \leq \chi < \infty$. The big bang singularity is $t = 0$ and the regular centre is $\chi = 0$. We have $q = 2/[3(1+k)]$ for a perfect fluid with $p = k\epsilon$ ($k > -1$), $q = 1/3$ for a massless scalar field ($k = 1$) and $q = 2/\lambda^2$ for a scalar field ϕ with the exponential potential $V = V_0 e^{-\sqrt{8\pi}\lambda\phi}$. The cosmic expansion is decelerated for $0 < q < 1$, accelerated for $q > 1$ and has constant speed for $q = 1$.

In terms of the conformal time η , defined by $ad\eta = dt$, we have $a \propto |\eta|^{q/(1-q)}$ for $q \neq 1$ and $a \propto e^{C\eta}$ for $q = 1$. The range of η is $0 < \eta < \infty$ for $0 < q < 1$, $-\infty < \eta < \infty$ for $q = 1$ and $-\infty < \eta < 0$ for $q > 1$. Defining new variables \hat{t} and \hat{r} by

$$\eta = \frac{1}{2} \left[\tan\left(\frac{\hat{t} + \hat{r}}{2}\right) + \tan\left(\frac{\hat{t} - \hat{r}}{2}\right) \right], \quad (\text{B2})$$

$$\chi = \frac{1}{2} \left[\tan\left(\frac{\hat{t} + \hat{r}}{2}\right) - \tan\left(\frac{\hat{t} - \hat{r}}{2}\right) \right], \quad (\text{B3})$$

we can draw the Penrose diagram for each case. Through this transformation, the big bang singularity $t = 0$ and the regular centre $\chi = 0$ are transformed respectively to $\hat{t} = 0$ and $\hat{r} = 0$ for $0 < q < 1$ and to $\hat{t} - \hat{r} = -\pi$ and $\hat{r} = 0$ for $q \geq 1$. It can be also shown [48] that future null infinity is given by $\hat{t} + \hat{r} = \pi$ for $0 < q \leq 1$ and $\hat{t} = 0$ for $q > 1$. The big bang singularity is spacelike for $0 < q < 1$ but null for $q \geq 1$.

When we introduce the double null coordinates

$$u = \eta - \chi, \quad v = \eta + \chi, \quad (\text{B4})$$

the line element takes the form

$$ds^2 = a^2[-dudv + \chi^2(d\theta^2 + \sin^2\theta d\phi^2)], \quad (\text{B5})$$

where

$$a^2 = C^{2/(1-q)} \left[(1-q) \left(\frac{u+v}{2} \right) \right]^{2q/(1-q)} \quad (\text{B6})$$

for $q \neq 1$ and

$$a^2 = C^2 e^{C(u+v)}, \quad (\text{B7})$$

for $q = 1$. The area radius r is given by $r = a(v-u)/2$. The Misner-Sharp mass m is written in this metric as

$$m = \frac{r}{2} \left(1 + \frac{4r_{,u}r_{,v}}{a^2} \right). \quad (\text{B8})$$

Then

$$\frac{2m}{r} = \left(\frac{q}{1-q} \right)^2 \left(\frac{v-u}{v+u} \right)^2, \quad (\text{B9})$$

for $q \neq 1$ and

$$\frac{2m}{r} = \frac{C^2}{4} (v-u)^2 \quad (\text{B10})$$

for $q = 1$. The past trapping horizon, which coincides with the cosmological apparent horizon, is given by $2m/r = 1$, or

$$u = (2q-1)v \quad (\text{B11})$$

for $q \neq 1$ and

$$v - u = \frac{2}{C}, \quad (\text{B12})$$

for $q = 1$. Therefore, the cosmological apparent horizon is spacelike for $0 < q < 1/2$, null for $q = 1/2$ and timelike for $q > 1/2$. Figure 6 shows five different Penrose diagrams, depending on the value of q . There is a particle horizon, given by $u = 0$, only for $0 < q < 1$. There is a cosmological event horizon, given by $v = 0$, only for $q > 1$. The flat Friedmann solution for $q = 1$ has neither a particle horizon nor a cosmological event horizon.

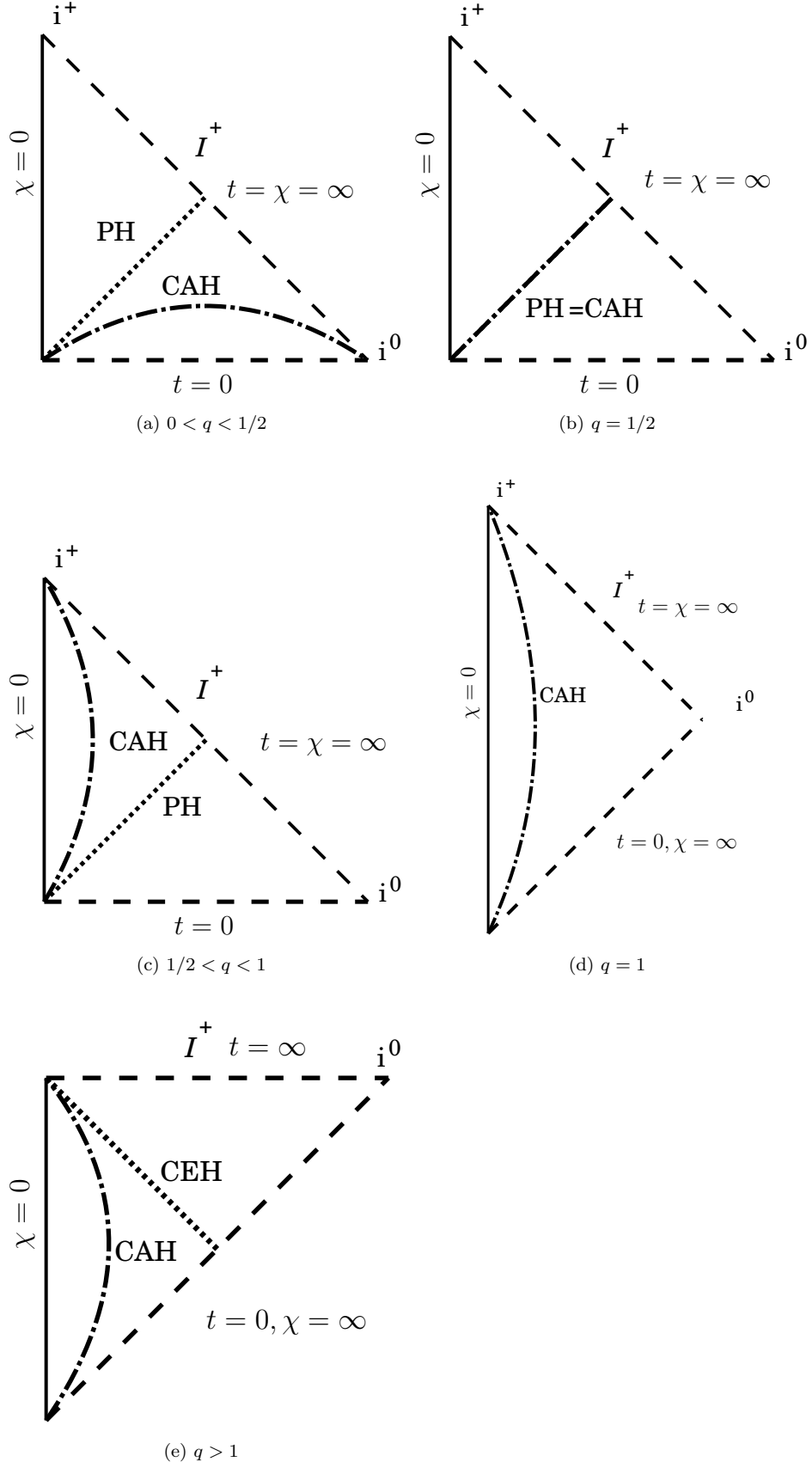


FIG. 6: The causal structure of the Friedmann universe with the scale factor $a \propto t^q$ for different values of q . The particle horizon (PH), cosmological apparent horizon (CAH) and cosmological event horizon (CEH) are indicated.

APPENDIX C: FRIEDMANN SOLUTION AS A SELF-SIMILAR SPACETIME

Although these flat Friedmann solutions are self-similar in the sense of homothety, it is not obvious in the present form. Using double-null coordinates, the standard form of spherically symmetric self-similar spacetimes is given by

$$ds^2 = -\tilde{a}^2(\sigma)d\tilde{u}d\tilde{v} + \tilde{u}\tilde{v}\tilde{b}^2(\sigma)(d\theta^2 + \sin^2\theta d\phi^2), \quad (\text{C1})$$

where $\sigma = \tilde{u}/\tilde{v}$ is the similarity variable. Since the metric with the double null coordinates u and v does not satisfy this form, we transform to new double null coordinates \tilde{u} and \tilde{v} .

For $q \neq 1$, \tilde{u} and \tilde{v} are given by

$$u = \pm|\tilde{u}|^{1-q}, \quad v = \pm|\tilde{v}|^{1-q}, \quad (\text{C2})$$

where the signs are chosen so that the sign of \tilde{u} (\tilde{v}) coincides with the sign of u (v) and we can show $-1 < \sigma \leq 1$. Then the metric functions become

$$\tilde{a}^2 = \text{const} \times \left| |\sigma|^{-(1-q)/2} \pm |\sigma|^{(1-q)/2} \right|^{2q/(1-q)}, \quad (\text{C3})$$

$$\begin{aligned} \tilde{b}^2 &= \text{const} \times \left| |\sigma|^{-(1-q)/2} \pm |\sigma|^{(1-q)/2} \right|^{2q/(1-q)} \\ &\times \left| |\sigma|^{-(1-q)} \mp |\sigma|^{(1-q)} \right|^2, \end{aligned} \quad (\text{C4})$$

where the upper and lower signs correspond to the positive and negative values of σ , respectively. For $q = 1$,

$$\tilde{u} = e^{Cu}, \quad \tilde{v} = e^{Cv} \quad (\text{C5})$$

and the metric functions become

$$\tilde{a}^2 = \text{const}, \quad (\text{C6})$$

$$\tilde{b}^2 = \text{const} \times (\ln \sigma)^2, \quad (\text{C7})$$

where $0 < \sigma \leq 1$.

The similarity surface is generated by a homothetic Killing vector. When this is null, it is called a similarity horizon and this does not depend on the choice of similarity variable. The induced metric on the similarity surface $\sigma = \text{const}$ is

$$\begin{aligned} ds^2 &= -\tilde{a}^2\sigma^{-1}d\tilde{u}^2 + \tilde{u}\tilde{v}\tilde{b}^2(d\theta^2 + \sin^2\theta d\phi^2) \\ &= -\tilde{a}^2\sigma d\tilde{v}^2 + \tilde{u}\tilde{v}\tilde{b}^2(d\theta^2 + \sin^2\theta d\phi^2). \end{aligned} \quad (\text{C8})$$

We provide two expressions because one of them may become invalid when one of the coordinates becomes degenerate. For $q \neq 1$, the only similarity horizon is $\sigma = 0$. This is outgoing and null for $0 < q < 1$, corresponding to the particle horizon $u = 0$, and ingoing and null for $q > 1$, corresponding to the cosmological event horizon $v = 0$. For $q = 1$, there is no similarity horizon and the similarity surfaces are $v - u = \text{const}$, which are timelike. The similarity horizon is important because it is the matching surface between the external Friedmann background and the internal self-similar solution.

APPENDIX D: ANALYSIS OF SIMILARITY HORIZON FOR THE MASSLESS CASE

We introduce a new independent variable u defined by

$$\frac{d\xi}{du} = 1 - 2z, \quad (\text{D1})$$

where the similarity horizon $\xi = \xi_s$ corresponds to $u = \pm\infty$ and is an equilibrium point. From Eqs. (3.7) – (3.9), we can write the ODEs near ξ_s in the form:

$$\frac{dz}{du} = z(1 - 2z)[2 - y^{-1}], \quad (\text{D2})$$

$$\frac{dy}{du} = (1 - 2z)[1 - (1 + 4\pi\gamma^2)y], \quad (\text{D3})$$

$$\frac{d\gamma}{du} = 2\kappa z - \gamma(y^{-1} - 2z), \quad (\text{D4})$$

together with the constraint given by Eq. (3.10). We now write the asymptotic solution near ξ_s as

$$z = \frac{1}{2}(1 + x_1), \quad y = y_s(1 + x_2), \quad \gamma = \gamma_s(1 + x_3), \quad \xi = \xi_s + x_4, \quad (\text{D5})$$

where y_s and γ_s are given by Eq. (3.25), and regard (x_1, x_2, x_3, x_4) as defining a 4-vector \mathbf{x} . The linearised ODEs can be written in the matrix form

$$\frac{d}{du}\mathbf{x} = \mathbf{A}\mathbf{x} \quad (\text{D6})$$

where

$$\mathbf{A} = \begin{pmatrix} \alpha - 1 & 0 & 0 & 0 \\ \alpha^{-1} - \alpha & 0 & 0 & 0 \\ 1 + \alpha & 1 + \alpha & -\alpha & 0 \\ -1 & 0 & 0 & 0 \end{pmatrix} \quad (\text{D7})$$

and $\alpha \equiv 4\pi\kappa^2$. This matrix generically has only two non-zero eigenvalues:

$$\lambda_1 = -1 + \alpha, \quad \lambda_2 = -\alpha. \quad (\text{D8})$$

These are associated with two eigenvectors

$$\mathbf{e}_1 = \begin{pmatrix} \alpha(1 - 2\alpha)(1 - \alpha) \\ -(1 - 2\alpha)(1 - \alpha)(1 + \alpha) \\ (1 - \alpha)(1 + \alpha) \\ \alpha(1 - 2\alpha) \end{pmatrix}, \quad \mathbf{e}_2 = \begin{pmatrix} 0 \\ 0 \\ 1 \\ 0 \end{pmatrix}, \quad (\text{D9})$$

and the two associated values of $\dot{\gamma}_s = (\gamma x_3/x_4)_s$ are given by Eq. (3.26). In particular, there is a solution belonging to the eigenvector \mathbf{e}_2 which has the form

$$z = \frac{1}{2}, \quad y = y_s, \quad \gamma = \gamma_s(1 \pm e^{-\alpha u}), \quad \xi = \xi_s, \quad (\text{D10})$$

and which we call a shock-wave solution. Note that the equilibrium point is a node for $\lambda_1 < 0$ and $\lambda_2 < 0$, with the primary direction being associated with the higher value, and a saddle for $\lambda_1 > 0$ and $\lambda_2 < 0$.

APPENDIX E: SIMILARITY HORIZON FOR THE MASSLESS CASE REVISITED

Here we revisit Brady's non-linear analysis of the similarity horizon for a massless scalar field [31]. We introduce new variables ζ and η such that

$$z = \frac{1}{2} + \zeta, \quad y = y_s + \eta, \quad y_s = \frac{1}{1 + 4\pi\kappa^2}, \quad (\text{E1})$$

where $\zeta = \eta = 0$ corresponds to the similarity horizon and only $\eta/\zeta \leq 0$ is allowed. When ζ and η are sufficiently small, Eqs. (3.7)-(3.10) reduce to

$$\gamma = -\kappa \pm \frac{1 + 4\pi\kappa^2}{\sqrt{8\pi}} \sqrt{-\frac{\eta}{\zeta}}, \quad (\text{E2})$$

$$\frac{d\eta}{d\zeta} = \pm \frac{2\sqrt{8\pi\kappa^2}}{1 - 4\pi\kappa^2} \sqrt{-\frac{\eta}{\zeta}} + \frac{1 + 4\pi\kappa^2}{1 - 4\pi\kappa^2} \frac{\eta}{\zeta}. \quad (\text{E3})$$

Here and throughout Appendix E the upper and lower signs correspond to the positive and negative branches in Eq. (E2). These equations can immediately be integrated to give

$$\sqrt{\frac{-\eta}{\zeta}} = \pm \frac{1}{\sqrt{2\pi\kappa}} + C|\zeta|^{4\pi\kappa^2/(1-4\pi\kappa^2)}, \quad (\text{E4})$$

$$\gamma = \frac{1}{4\pi\kappa} \pm \frac{C(1 + 4\pi\kappa^2)}{\sqrt{8\pi}} |\zeta|^{4\pi\kappa^2/(1-4\pi\kappa^2)}, \quad (\text{E5})$$

where C is an integration constant. If $\zeta < 0$ and $\eta > 0$, Eq. (E4) with the upper sign coincides with Brady's solution (Eq. (C6) in [31]), except for the exponent of the second term on the right-hand side, which may be a typographical error. The negative-branch solutions do not cross the similarity horizon $\zeta = \eta = 0$.

The solution with the upper sign has the following behaviour. If $C = 0$, it always crosses the similarity horizon. For $0 < 4\pi\kappa^2 < 1$, there is a one-parameter family of solutions which cross the similarity horizon, because the second term on the right-hand side of Eqs. (E4) and (E5) goes to zero as $\zeta \rightarrow 0$. For $4\pi\kappa^2 > 1$, however, the solution with $C = 0$ is isolated because η will not go to zero as $\zeta \rightarrow 0$ if $C \neq 0$. If we consider the derivatives along solutions with $C \neq 0$, because of the second term, $d\gamma/d\zeta$ is diverging for $0 < 4\pi\kappa^2 < 1/2$ and finite for $1/2 < 4\pi\kappa^2 < 1$. This reflects the behaviour of sound-wave solutions with $C \neq 0$, which is discussed in Section III E using the linearised ODEs. Note that the shock-wave solution, which is given by Eq. (D10), now has $\eta = \zeta = 0$ but changing γ .

APPENDIX F: ANALYSIS OF SIMILARITY HORIZON FOR THE POTENTIAL CASE

Using the variable u defined by Eq. (D1), the system of ODEs near the similarity horizon has the form:

$$\frac{dz}{du} = z(1 - 2z)[2 - y^{-1}(1 - \beta)], \quad (\text{F1})$$

$$\frac{dy}{du} = (1 - 2z)[1 - \beta - (1 + 4\pi\gamma^2)y], \quad (\text{F2})$$

$$\frac{d\gamma}{du} = 2\kappa z - \gamma[y^{-1}(1 - \beta) - 2z] + \frac{\beta}{4\pi\kappa y}, \quad (\text{F3})$$

$$\frac{d\beta}{du} = 2(1 - 2z)\beta(1 + \gamma/\kappa), \quad (\text{F4})$$

together with the constraint

$$1 - \beta = y[(1 + 4\pi\kappa^2) - 4\pi(\gamma + \kappa)^2(1 - 2z)]. \quad (\text{F5})$$

The nature of the equilibrium point can again be classified by the behaviour of solutions there. We put

$$z = \frac{1}{2}(1 + x_1), \quad y = y_s(1 + x_2), \quad \gamma = \gamma_s(1 + x_3),$$

$$\xi = \xi_s + x_4, \quad \beta = \beta_s(1 + x_5),$$

where x_1 to x_5 are regarded as components of a 5-vector \mathbf{x} . From the regularity condition at the similarity horizon associated with Eq. (F3) and the constraint equation (F5), we obtain Eq. (4.14), so that the similarity horizon is parametrized by the values of κ and β_s .

We now write the linearised ODEs in the form:

$$\frac{d}{du} \mathbf{x} = \mathbf{A} \mathbf{x}, \quad (\text{F6})$$

where the matrix \mathbf{A} is given by

$$\mathbf{A} = \begin{pmatrix} \alpha - 1 & 0 & 0 & 0 & 0 \\ A_{21} & 0 & 0 & 0 & 0 \\ A_{31} & A_{32} & -\alpha & 0 & A_{35} \\ -1 & 0 & 0 & 0 & 0 \\ A_{51} & 0 & 0 & 0 & 0 \end{pmatrix} \quad (\text{F7})$$

with

$$A_{21} = \frac{(1 + \alpha)[\beta_s(1 + \alpha^2) + \alpha(1 - \alpha)]}{\alpha^3(1 - \beta_s)^2} \times [(1 - \alpha)\beta_s + \alpha], \quad (\text{F8})$$

$$A_{31} = A_{32} = \frac{(1 + \alpha)[(1 - \alpha)\beta_s + \alpha]}{\beta_s + \alpha}, \quad (\text{F9})$$

$$A_{35} = \frac{\beta_s(1 + \alpha)[(1 - \alpha)\beta_s + 2\alpha]}{(1 - \beta_s)(\beta_s + \alpha)}, \quad (\text{F10})$$

$$A_{51} = -\frac{2(1 + \alpha)[(1 - \alpha)\beta_s + \alpha]}{\alpha^2(1 - \beta_s)}, \quad (\text{F11})$$

where $\alpha \equiv 4\pi\kappa^2$. This matrix has three zero eigenvalues and two generically non-zero ones, $\lambda_1 = -1 + \alpha$ and $\lambda_2 = -\alpha$. Two of the eigenvectors associated with zero eigenvalues do not satisfy the constraint equation and so are ruled out. The eigenvectors associated with the eigenvalues λ_1, λ_2 are respectively

$$\mathbf{e}_1 = \begin{pmatrix} 1 - \alpha \\ (e_1)^2 \\ (e_1)^3 \\ 1 \\ (e_1)^5 \end{pmatrix}, \quad \mathbf{e}_2 = \begin{pmatrix} 0 \\ 0 \\ 1 \\ 0 \\ 0 \end{pmatrix}, \quad (\text{F12})$$

where

$$(e_1)^2 = -\frac{(1+\alpha)[(1+\alpha^2)\beta_s + \alpha(1-\alpha)]}{\alpha^3(1-\beta_s)^2} \times [(1-\alpha)\beta_s + \alpha], \quad (\text{F13})$$

$$(e_1)^3 = \frac{(1+\alpha)[(1-\alpha)\beta_s + \alpha]Q}{\alpha^3(1-\beta_s)^2(1-2\alpha)(\beta_s + \alpha)}, \quad (\text{F14})$$

$$Q \equiv -(1-\alpha)(\alpha^2 + \alpha - 1)\beta_s^2 - 2\alpha(\alpha^2 + 2\alpha - 1)\beta_s + \alpha^2(1-\alpha), \quad (\text{F15})$$

$$(e_1)^5 = \frac{2(1+\alpha)[(1-\alpha)\beta_s + \alpha]}{\alpha^2(1-\beta_s)}. \quad (\text{F16})$$

These eigenvectors lie on the constraint surface.

-
- [1] S. Hawking, *Mon. Not. R. Astron. Soc.* **152**, 75 (1971).
[2] B. J. Carr, *Astrophys. J.* **201**, 1 (1975).
[3] B. J. Carr, in *The Future of Theoretical Physics and Cosmology*, p 236, ed. G. Gibbons, P. Shellard & S. Rankine, (Cambridge University Press, 2003) .
[4] R. Bean and J. Magueijo, *Phys. Rev.* **D66**, 063505 (2002).
[5] P. S. Custodio and J. E. Horvath, *Int. J. Mod. Phys.* **D14**, 257 (2005).
[6] J. Kormendy and D. Richstone, *Ann. Rev. Astron. Astrophys.* **33**, 581 (1995).
[7] Ya. B. Zeldovich and I. D. Novikov *Sov. Astron.* **10**, 602 (1967).
[8] B. J. Carr and S. W. Hawking, *Mon. Not. R. Astron. Soc.* **168**, 399 (1974).
[9] T. Harada and B. J. Carr, *Phys. Rev.* **D71**, 104009 (2005).
[10] E. Babichev, V. Dokuchaev, Yu. Eroshenko, *Phys. Rev. Lett.* **93**, 021102 (2004).
[11] S. Nojiri and S. D. Odintsov, *Phys. Rev.* **D70**, 103522 (2004).
[12] E. Babichev, V. Dokuchaev, Yu. Eroshenko, *J. Exp. Theor. Phys.* **100**, 528 (2005).
[13] A. V. Frolov, *Phys. Rev.* **D70**, 061501(R) (2004).
[14] S. Mukohyama, *Phys. Rev.* **D71**, 104019 (2005).
[15] B. J. Carr, Ph.D. thesis, Cambridge University (1976).
[16] G. V. Bicknell and R. N. Henriksen, *Astrophys. J.* **225**, 237 (1978).
[17] B. J. Carr and A. Yahil, *Astrophys. J.* **360**, 330 (1990).
[18] D. K. Nadezhin, I. D. Novikov and A. G. Polnarev, *Sov. Astron.* **22**, 129 (1978).
[19] I. D. Novikov and A. G. Polnarev, *Sov. Astron.* **24**, 147 (1980).
[20] J. C. Niemeyer and K. Jedamzik, *Phys. Rev.* **D59**, 124013 (1999).
[21] K. Jedamzik and J. C. Niemeyer, *Phys. Rev.* **D59**, 124014 (1999).
[22] M. Shibata and M. Sasaki, *Phys. Rev.* **D60**, 084002 (1999).
[23] I. Hawke and J. M. Stewart, *Classical Quantum Gravity* **19**, 3687 (2002).
[24] I. Musco, J. C. Miller and L. Rezzola, *Classical Quantum Gravity* **22**, 1405 (2005).
[25] H. Maeda, J. Koga and K. Maeda, *Phys. Rev.* **D66**, 087501 (2002).
[26] D. N. C. Lin, B. J. Carr and S. M. Fall, *Mon. Not. R. Astron. Soc.* **177**, 51 (1976).
[27] G. V. Bicknell and R. N. Henriksen, *Astrophys. J.* **219**, 1043 (1978).
[28] M. S. Madsen, *Classical Quantum Gravity* **5**, 627 (1988).
[29] T. Harada and B. J. Carr, *Phys. Rev.* **D71**, 104010 (2005).
[30] T. Harada and B. J. Carr, *Phys. Rev.* **D72**, 044021 (2005).
[31] P. R. Brady, *Phys. Rev.* **D51**, 4168 (1995).
[32] T. Harada and H. Maeda, *Classical Quantum Gravity* **21**, 371 (2004).
[33] B. J. Carr and C. Gundlach, *Phys. Rev.* **D67**, 024035 (2003).
[34] A. Ori and T. Piran, *Phys. Rev.* **D42**, 1068 (1990).
[35] D. Christodoulou, *Commun. Math. Phys.* **105**, 337 (1986); **106**, 587 (1986); **109**, 591 (1987); **109**, 613 (1987).
[36] M. D. Roberts, *Gen. Relat. Grav.* **21**, 907 (1989).
[37] S. A. Hayward, gr-qc/9303006.
[38] S. A. Hayward, *Phys. Rev.* **D53**, 1938 (1996).
[39] T. Harada, *Classical Quantum Gravity* **18**, 4549 (2001).
[40] P. C. Vaidya, *Proc. Indian Acad. Sci.* **A33**, 264 (1951); *Nature* **171**, 260 (1953).
[41] J. Wainwright and G. F. R. Ellis, *Dynamical Systems in Cosmology* (Cambridge University Press, 1997).
[42] H. Maeda and T. Harada, *Phys. Lett.* **B607**, 8 (2005).
[43] H. Maeda, T. Harada and B. J. Carr, (unpublished).
[44] A. A. Coley, *Classical Quantum Gravity* **14**, 87 (1997).
[45] H. Maeda and T. Harada, in *General Relativity Research Trends. Horizons in World Physics, Volume 249*, ed. R. Albert (Nova Science Publishers, New York, 2005).
[46] T. Jacobson, *Phys. Rev. Lett.* **83**, 2699 (1999).
[47] E. Bettwieser and W. Glatzel, *Astron. Astrophys.* **94**, 306 (1981).
[48] J. M. M. Senovilla, *Gen. Relativ. Grav.* **30**, 701 (1998).